PNAS RESEARCH ARTICLE | GENETICS

Environmental radiation exposure at Chornobyl has not systematically affected the genomes or chemical mutagen tolerance phenotypes of local worms

Sophia C. Tintori[a,1], Derin Çağlar[a], Patrick Ortiz[a], Ihor Chyzhevskyi[b], Timothy A. Mousseau[c], and Matthew V. Rockman[a,1]

Edited by Rodney Rothstein, Columbia University, New York, NY; received August 28, 2023; accepted January 18, 2024

The 1986 disaster at the Chornobyl Nuclear Power Plant transformed the surrounding region into the most radioactive landscape known on the planet. Whether or not this sudden environmental shift selected for species, or even individuals within a species, that are naturally more resistant to mutagen exposure remains an open question. In this study, we collected, cultured, and cryopreserved 298 wild nematode isolates from areas varying in radioactivity within the Chornobyl Exclusion Zone. We sequenced and assembled genomes de novo for 20 *Oscheius tipulae* strains, analyzed their genomes for evidence of recent mutation acquisition in the field, and observed no evidence of an association between mutation and radioactivity at the sites of collection. Multigenerational exposure of each of these strains to several chemical mutagens in the lab revealed that strains vary heritably in tolerance to each mutagen, but mutagen tolerance cannot be predicted based on the radiation levels at collection sites, and Chornobyl isolates were not systematically more resistant than strains from undisturbed habitats. In sum, the absence of mutational signatures does not reflect unique capacity for tolerating DNA damage.

Chornobyl | rhabditids | mutagen tolerance

Significance

Environmental contamination from nuclear accidents poses immediate health risks, but it is less clear what the long-term heritable effects on local populations are, either in terms of systematic genome changes or specific adaptations. Here, we collected nematodes from high- and low-radioactivity areas of the Chornobyl Exclusion Zone and sequenced their genomes, showing that there are no detectable changes to the high-radiation animals' genomes broadly. We also developed an assay to measure sensitivity to chronic chemical mutagen exposure in the lab, showing that there is heritable variation in wild isolates' tolerance to various forms of DNA damage, but it is not associated with radiation exposure in the field.

Mutagens—whether endogenous or exogenous, naturally occurring or anthropogenic—are a ubiquitous presence in our environment. Of the tens of thousands of DNA lesions formed on average in each human nucleus each day, the vast majority are corrected by our DNA repair machinery without incident. Even so, it is well established that heritable genetic variants in DNA repair components can contribute to cancer, birth defects, premature aging, and neurological defects (1, 2).

The Chornobyl Exclusion Zone (CEZ), the site of the largest nuclear disaster in history, presents an opportunity to test whether chronic radiation exposure selects for an adaptive response in DNA repair mechanisms or mutagen tolerance more broadly. Nematodes are an ideal animal system for such an investigation, as they can reliably be collected from a broad range of environments (3–5), their small genomes and short generation times suit them to experimental genetics and studies of natural variation (3, 6–8), and hypotheses generated in the field can be tested directly in the lab.

Areas of the CEZ that are easily accessible to wildlife reach tens of sieverts per year, a level of radiation that is an order of magnitude higher than those encountered during space travel (*SI Appendix*, Fig. S1). Though animals can be found in these high radiation areas, evidence suggests that the exclusion zone may be a population sink, at least for more mobile species (9), making it difficult to say how far back in an animal's lineage they might have been exposed to these levels of radiation.

In recent years, ecological studies in the CEZ have reported species with abnormal physiology (10, 11), putatively due to radiation-induced DNA damage. Meanwhile, genetic studies have shown mixed evidence for detectable signatures of radiation damage in the genomes of surviving animals (12–18). To be clear, a lack of a recognizable mutagenic signature, or a lack of detectable selection pressure on tolerance alleles, does not suggest a harm-free environment. For example, it is both true that a recent study revealed no increase in de novo germline mutation rates in exposed parents who conceived after the disaster (18) and also that an untold number developed cancer due to their exposure. Thirty-eight years after the disaster, researchers still strive to understand the extent and the implications of the damage done to life in this area.

In our study, we collected nematode worms from locations throughout the CEZ ranging in ambient radiation levels from innocuous to dangerous. We use isohermaphrodite lines descended from these isolates for complementary experiments—first interrogating the genomes for genetic evidence of exposure in recent history and then experimentally testing their relative mutagen tolerance in a controlled setting.

Author affiliations: [a]Department of Biology and Center for Genomics & Systems Biology, New York University, New York, NY 10003; [b]Department of Coordination of International Projects of the State Specialized Enterprise "Ecocentre", Kyiv 01133, Ukraine; and [c]Department of Biological Sciences, University of South Carolina, Columbia, SC 29208

Preprint server: An earlier version of this manuscript was published on bioRxiv, DOI: 10.1101/2023.05.28.542665.

Author contributions: S.C.T. and M.V.R. designed research; S.C.T., D.Ç., P.O., I.C., T.A.M., and M.V.R. performed research; S.C.T. analyzed data; and S.C.T. and M.V.R. wrote the paper.

The authors declare no competing interest.

This article is a PNAS Direct Submission.

[1]To whom correspondence may be addressed. Email: sophia.tintori@nyu.edu or mrockman@nyu.edu.

This article contains supporting information online at https://www.pnas.org/lookup/suppl/doi:10.1073/pnas.2314793121/-/DCSupplemental.

Published March 5, 2024.

Results

Rhabditids from Chornobyl Substrates Span More than Three Orders of Magnitude in Ambient Radioactivity at Collection Sites. During two collecting trips to the CEZ, in August and October of 2019, we collected 237 local substrates (124 fruit, 65 soil and leaf litter, 18 invertebrates, 15 compost, 13 riparian plant stems, 1 wolf fecal sample, and 1 mushroom), as well as 16 substrates (apple and tomato) we placed as bait and returned to collect days later. We recovered nematodes from 157 of these substrates and extracted 748 nematode isolates to establish cultures on nematode growth medium with *E. coli* as food source. We successfully established cultures for 298 of these isolates, representing 118 of the substrates collected, and we cryopreserved them for subsequent analysis. Isolates that failed to establish permanent stocks included non-bacterivorous species that could not proliferate on *E. coli*, unmated females from dioecious species, and cultures that did not survive repeated cryopreservation attempts. In a few cases, nematophagous bacteria or fungi isolated with the worms killed them before they could reproduce. Ambient radiation at collection sites ranged from 2 to 4,786 mSv/y, as measured by Geiger counter (Fig. 1*A*), and substrates ranged from 0 to 2,019 Bq/gram dry weight, as measured by gamma spectrometer (*SI Appendix*, Fig. S2). Ambient radiation and substrate radioactivity were linearly related when separated by substrate type, with soil substrates averaging 30 to 100× higher radioactivity than fruit substrates from the same collection site (*SI Appendix*, Fig. S2).

To identify each cultured isolate, we sequenced a ~518-bp fragment of the 18S rDNA gene. All worms belong to Rhabditida, with representatives from *Acrobeloides*, *Mesorhabditis*, *Oscheius*, *Panagrellus*, *Panagrolaimus*, *Pristionchus*, *Pelodera*, and *Rhabditis* (Fig. 1*B*). *Acrobeloides* were found more frequently in the drier and higher ambient-radiation environments, while *Panagrolaimus* and *Oscheius* were isolated from a broad range of radiation and moisture levels (Fig. 1*C*).

Of the three taxa we collected in the highest numbers, *Oscheius* was found in a broad range of environmental conditions (Fig. 1*B*) and geographic locations (*SI Appendix*, Fig. S3), missing only in the highest radiation sites we sampled, which were also drier than its typical habitat. Of all the isolates we collected, *Oscheius* is also the best characterized as a research model, and its *Caenorhabditis elegans*–like androdioecious mating system and 5-d life cycle make it highly amenable to genetic analysis. By contrast, *Acrobeloides*, which we collected from higher radiation environments, is obligately parthenogenetic and has a generation time of about 30 d (4, 20, 21). For these reasons, we chose the *Oscheius* isolates to investigate further.

De Novo Genome Assemblies of *Oscheius tipulae* from Chornobyl Reveal No Genome Rearrangements. To test whether the genomes of worms from Chornobyl carry signatures of living in a mutagenic environment, we selected 20 *O. tipulae* for genome sequencing—15 from the CEZ and 5 previously collected from other regions (Philippines, Germany, United States, Mauritius,

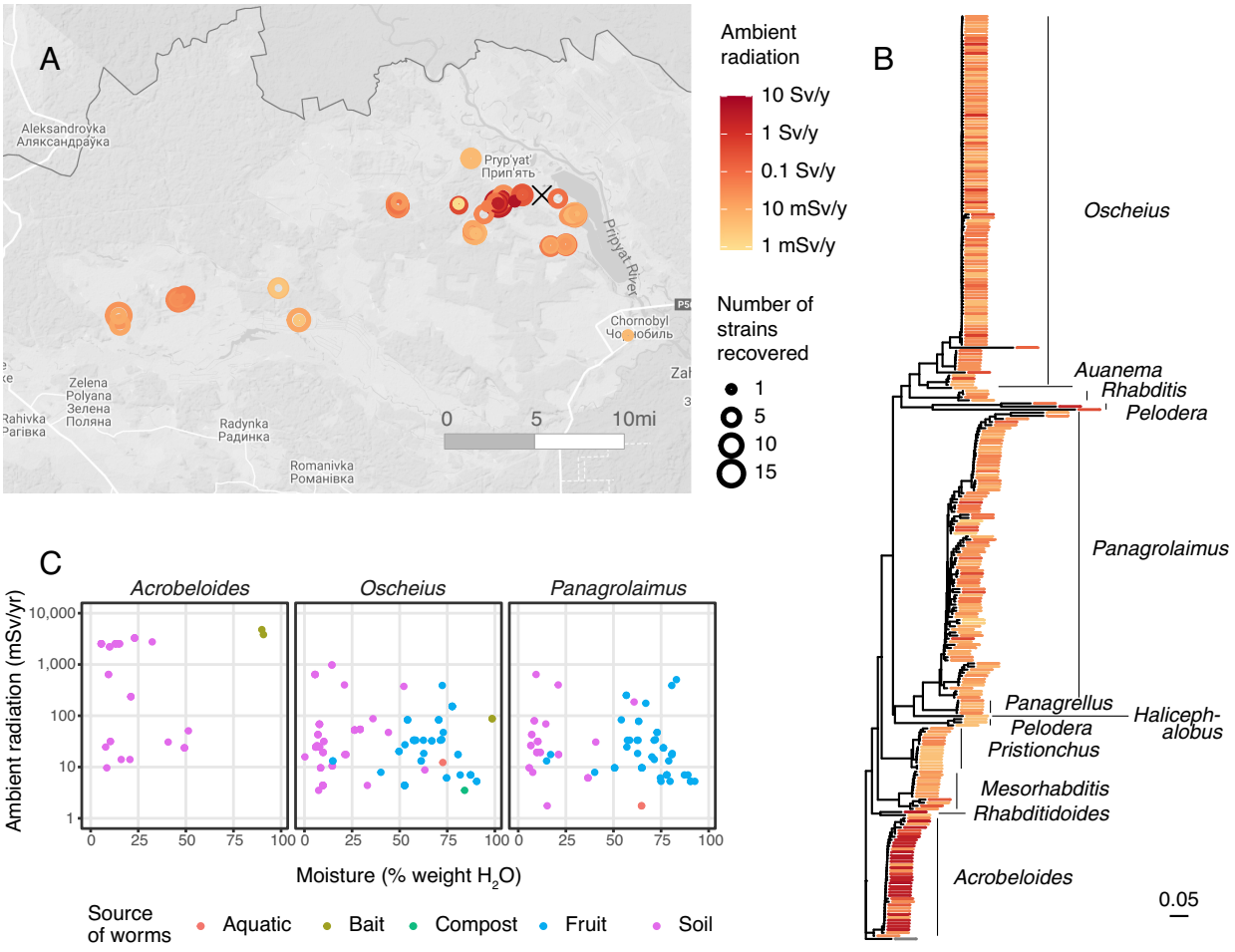

Fig. 1. 298 nematode lines collected, identified, and cryopreserved from the CEZ. (*A*) Sites from which substrates were collected. Circle size represents the number of nematode strains collected and successfully cryopreserved. Colors represent ambient radiation at each site at the time of collection. Map generated with ggmap (19) using Google Maps data (*B*) Neighbor-joining tree for a 518-bp segment 18S rDNA from 298 cryopreserved nematode strains. Branch lengths represent the proportion of sites that differ. (*C*) Environmental conditions at collection sites of the three most abundant taxa.

and Australia). The 15 CEZ strains were selected (from a total of 120 *O. tipulae* isolates recovered from 53 unique sites) to represent a broad range of geographic locations and ambient radiation backgrounds, ranging from 3.5 to 978.3 mSv/y, across a distance of 50 km. Additionally, we sequenced and assembled the genome of the JU75 strain of *O. sp. 3,* the sister species to *O. tipulae* (22), to use as an outgroup in some of our subsequent analyses.

We performed long-read sequencing to facilitate de novo genome assembly, as well as short-read sequencing to polish the assembled genomes. For the 20 de novo genomes, the average N50 was 9.14 Mb (median = 9.64 Mb, range = 5.85 Mb to 10.06 Mb), compared to the reference genome's N50 of 10.82 Mb (21). *O. tipulae* hermaphrodites reproduce primarily by self-fertilization and so are virtually homozygous, simplifying the genome assembly process.

Strains from Chornobyl are all genetically closer to each other than to the non-Chornobyl strains, with the exception of DF5103 from Berlin which clusters with the Chornobyl strains (Fig. 2). Genetic distance between strains is correlated with geographic distance when compared across all strains, but not when compared among Chornobyl strains only (Mantel test with 999 replicates, observation = 0.930 and –0.021, *P* value = 0.001 and 0.478 for all samples and CEZ-only samples respectively, *SI Appendix*, Fig. S4). Variants are distributed unevenly across the genome, with higher polymorphism in chromosome arms than centers (*SI Appendix*, Fig. S5). Linkage disequilibrium drops off quickly (within 50 bases) but then plateaus around r^2 = 0.4, reflecting a high rate of self-fertilization in this androdiecious species, while also suggesting that a low but nonnegligible rate of outcrossing [~10^{-3} to 10^{-6}/generation, (23)] does occur in the wild (*SI Appendix*, Fig. S6).

Because ionizing radiation can cause double-strand breaks in DNA, leading to rearrangements when resolved by non-homology-based mechanisms, we tested whether isolates from Chornobyl exhibited heritable chromosomal rearrangements. We generated synteny plots between the published reference genome (21) and each de novo genome (Fig. 3). These synteny plots revealed no evidence of chromosome rearrangements compared to the reference genome, with the exception of a 2 Mb inversion on the left arm of chromosome V in non-Chornobyl strain DF5111 from Australia.

Differences in contig number between assemblies are explained by long-read coverage (*SI Appendix*, Fig. S7), suggesting that instances of low contiguity for some samples are artifacts of sequencing and not evidence of wide-spread chromosomal fission events. We observed a region of low synteny on the left arm of chromosome V; possible explanations include mobile sequences in all strains, rearrangements unique only to reference strain CEW1, or poor alignment in this region of the genome. Pairwise comparisons between every combination of genomes reveal similar patterns (example in *SI Appendix*, Fig. S8), excluding the possibility that this is a CEW1-exclusive phenomenon. This region is coincident with the highest density of repeats in the genome (21), strengthening the hypothesis that the low synteny is due to assembly errors. We inspected assemblies by eye to confirm that synteny breaks were not associated with assembly errors, and ultimately we conclude that the low synteny in this region is likely real, and possibly caused by the high density of repeats (*SI Appendix*, Fig. S9). The assembly gap on the right side of chromosome V in all assemblies coincides with the long repetitive rDNA cluster.

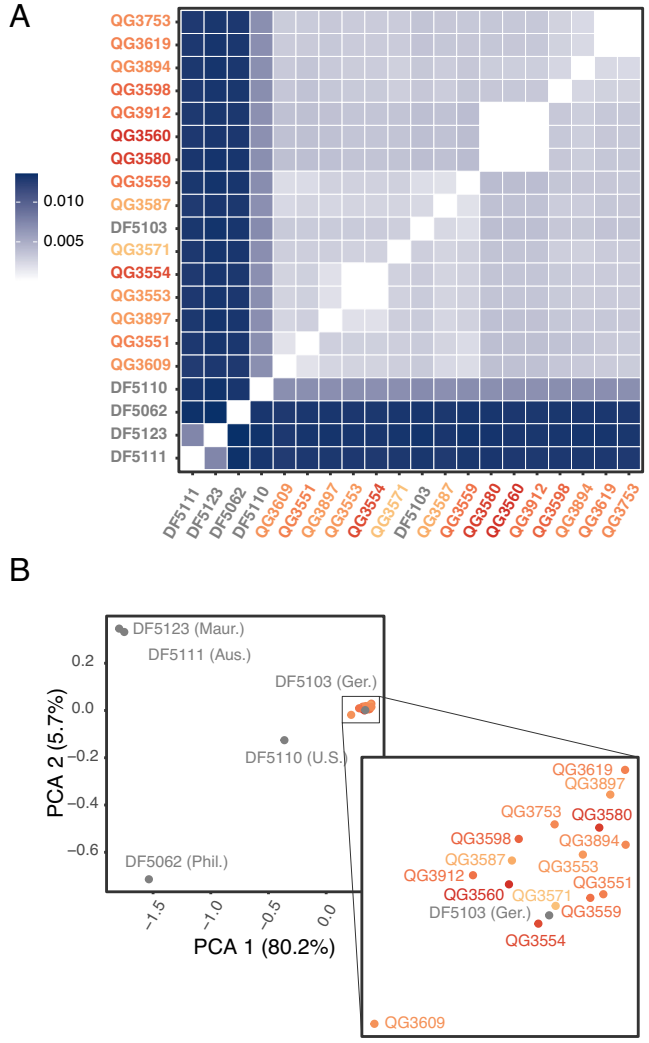

Fig. 2. Population structure of 20 *O. tipulae* strains sequenced. (*A*) Genetic distances between each pair of samples. Values represent the frequency of differences between the two strains. (*B*) PCA of all 20 *O. tipulae* genomes. Inset shows detail of the Chornobyl and Berlin cluster. "DF" strains were collected previously, radioactivity unknown, from the Philippines (DF5062), Germany (DF5103), the United States (DF5110), Australia (DF5111), and Mauritius (DF5123).

Recent Mutations Are Comparable between Worms from High- and Low-Radioactivity Areas. Having found no evidence of large-scale chromosomal rearrangements in Chornobyl genomes, we next looked for signs that nematodes collected from higher radiation environments might have larger numbers of recently acquired mutations due to environmental exposure. To isolate recent mutations while accounting for variation in genealogy among strains and along the genome, we employed a tree-based method to compare two ingroup strains at a time, using an outgroup to assign recent mutations between the pair to either branch (Fig. 4*A*).

We aligned two *O. tipulae* genomes at a time to the genome of an outgroup, allowing us to count the number of mutations unique to each of the two strains, accounting for variation in coalescence times along the genome. We define "relative mutation acquisition" as the ratio between these two unique mutation counts (Fig. 4*A*). The goal of this approach is to disregard most differences each strain carries compared to the outgroup, and only count mutations acquired during recent divergence and whose ancestral allele can be determined from the outgroup, and then finally to report how much faster or slower one strain has acquired mutations compared to the other during the same period of unshared history.

Though *Oscheius sp. 3* is the closest known outgroup species, only 5 to 10% of the sites in each *O. tipulae* genome aligned to *O. sp. 3* genome. The *O. sp. 3* genome therefore is a mixture of conserved sites, likely under strong purifying selection, and sites that differ from *O. tipulae* by multiple substitutions; both factors

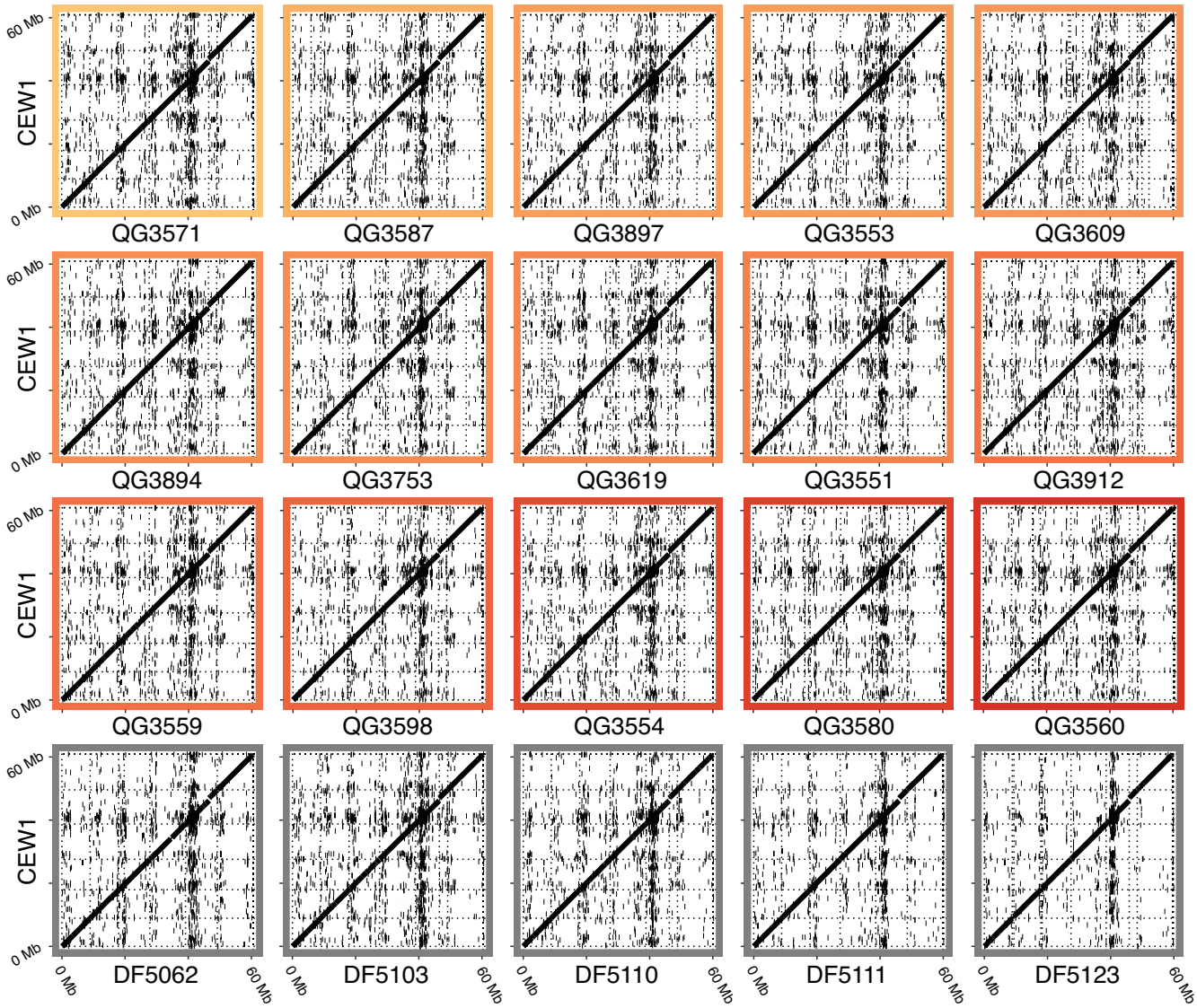

Fig. 3. Synteny plots of each newly assembled *O. tipulae* wild isolate genome compared to the CEW1 reference genome. Border color reflects radioactivity at the collection site, using the same color scale as in Fig. 1. Horizontal dotted lines delineate the six CEW1 chromosomes, and vertical dotted lines delineate the contigs of each new assembly. Stretches of alignment are plotted as lines that, due to the scale of the plot, are wider than they are long.

reduce the utility of *O. sp. 3* as an outgroup. We therefore adopted an intraspecific outgroup approach, using *O. tipulae* DF5123 from Mauritius as our outgroup genome but limiting analysis to pairwise comparisons between European strains—a tight genetic cluster distant from DF5123 (Fig. 2*B*)—and excluding genomic regions with genealogies inconsistent with an outgroup position for DF5123. With this intraspecific approach, 87 to 89% of the genome aligned to the *O. tipulae* reference, and 78% of aligned variants fell within regions consistent with the desired genealogy.

In this way, we generated 15 relative mutation acquisition values for each strain—one value for each comparison to the other strains (as an example, all 15 pairwise comparisons using strain QG3571 in the numerator are shown in Fig. 4*B*). We hypothesized that worms from higher radiation environments might have acquired more mutations in recent history than worms from lower radiation environments within the CEZ. Based on these 16 isolates (15 from Chornobyl and one from Berlin), we found no significant association between average relative mutation acquisition and radioactivity at the time of collection (P = 0.187 for ambient radioactivity by Geiger counter, P-value = 0.708 for substrate radioactivity by gamma spectrometer) for the nuclear genome (Fig. 4*C*) or the mitochondrial genome (P = 0.356 for ambient, P = 0.818 for substrate). Comparing relative mutation acquisition to fold-change difference in ambient radiation levels between each pair using the Mantel test also revealed no association (P = 1), and subdividing data by mutation type also revealed no significant relationships (*SI Appendix*, Fig. S10). We used simulations to estimate our power to detect elevated mutation acquisition, conditional on the sample genealogy and observed number of variants. If the highest radiation levels in this study caused the annual mutation rate to increase twofold during the 33 y between the reactor explosion and our collections, we estimate 23% power to detect the effect, 65% power to detect a fivefold mutation rate increase, and 98.4% power for a 10-fold increase.

To test whether the Chornobyl strains differed systematically from non-Chornobyl *O. tipulae*, we repeated the analysis using all 20 sequenced strains with *O. sp. 3* as the outgroup, despite the limitations of this species as an outgroup, as outlined above. We saw no evidence of any significant difference in mutation acquisition between CEZ and non-CEZ strains (*SI Appendix*, Fig. S11). Given the small and evolutionarily constrained fraction of the genome we were able to analyze, we consider this result inconclusive, and the

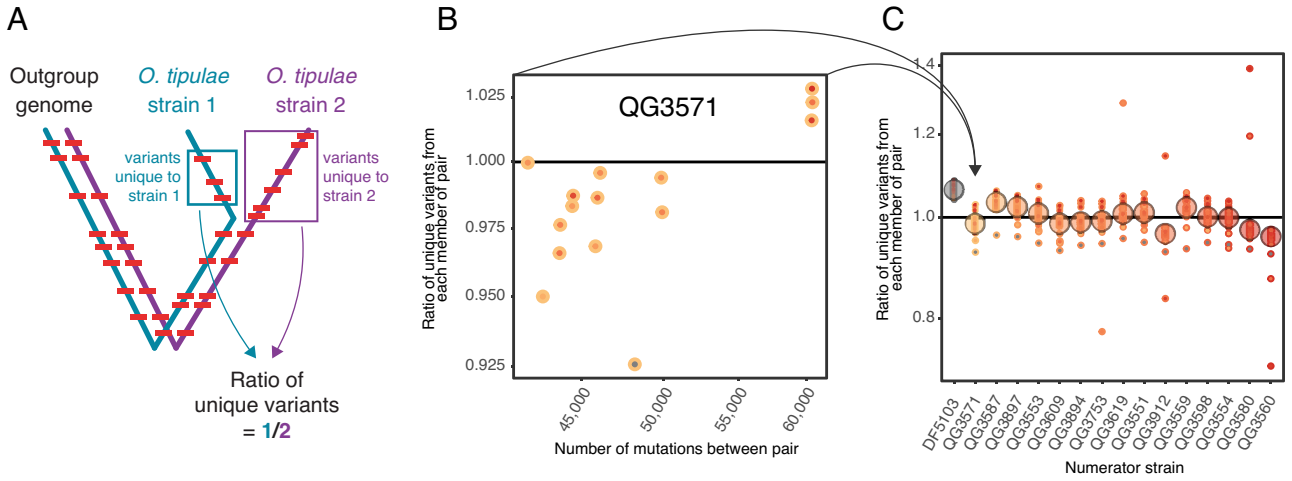

Fig. 4. Relative mutation acquisition in *O. tipulae* wild isolates. (*A*) Schematic for calculating mutation acquisition for one isolate (strain 1) relative to another (strain 2). (*B*) Relative mutation acquisition for strain QG3571 when compared to each of the other 15 strains, for example. These values are collapsed on the *x*-axis and summarized on the *y*-axis for each strain in the next panel. (*C*) Median relative mutation acquisition for each strain (*P*-value for glm testing association of median relative mutation acquisition to radioactivity = 0.187). Large circles are the median, and small circles are each pairwise comparison. The *y*-axis is plotted with a log transformation; tick labels report prelogged values. The color scheme matches that in Fig. 1.

earlier results from the German strain DF5103 (Fig. 4*C*) provide the strongest evidence that Chornobyl strains lack signatures of elevated mutation accumulation. Replicating these analyses using tandem repeat variants similarly revealed no association between mutation frequency and radioactivity at the site of collection.

The *O. tipulae* strains we sequenced include some that are very closely related to one another (0.025% divergence, compared to the range of 0.17 to 1.35% of all other samples). Of the approximately 2,500 variants that differ between each of these pairs, two sets have a striking imbalance in how the variants are distributed: Among the 2,475 mutations differing between QG3580 and QG3560, they are disproportionately distributed at a ratio of 1.46:1 (binomial distribution P-value=10^{-20}), and the 2,881 sites that differ between QG3619 and QG3753 are distributed 1.28:1 (P-value = 3×10^{-11}). The strong difference in recent mutation acquisition between these closely related strains is intriguing, but it is unclear whether this effect is caused by demographic differences, differences in exposure history, or differences in each strain's physiological response to mutagenesis. Differences in mutation spectrum between high and low mutation acquisition strains may suggest one mechanism over another, so we analyzed the similarities of each of these four mutation spectra to COSMIC signatures (24), but because there are only two pairs of highly similar strains, we were not able to determine the statistical significance of these trends (*SI Appendix*, Fig. S12). We were able to test our final hypothesis—whether strains have different physiological responses to mutagen exposure—in the lab using our cryopreserved cultures of each of these strains.

***O. tipulae* Strains Exhibit Heritable Variation in Their Response to Mutagen Exposure, Which Is Not Explained by Radioactivity at Sites of Collection.** The result described above, that *O. tipulae* strains vary in their recent mutation acquisition but not based on their inferred radiation exposure, raises two questions that are testable via controlled experiments in the lab. First, why are Chornobyl *O. tipulae* no more mutated than non-Chornobyl *O. tipulae*? Is it because the level of radiation that they were exposed to was not challenging to the physiology typical of *O. tipulae*, or is it because the strains that thrive in Chornobyl are specifically more resilient to mutagens than other strains of the same species? Second, for the strains that do have fewer mutations in their recent history, as observed in the pairs described at the end of the last section, is it because they are more resistant to mutagenesis? Our cryopreserved cultures allow us to test these models directly. We tested isogenic descendants of the 20 natural strains of *O. tipulae* described above for their tolerance to mutagen exposure in the lab.

Motivated by previous experiments that showed reduced spermatogenesis to be the first dramatic fitness effects of ionizing radiation exposure (25), we developed a chronic mutagen tolerance assay that spans the entire lifecycle multiple times. We adapted the *C. elegans* Lifespan Machine method (26) to build an assay in which an isogenic population of worms is allowed to grow undisturbed for 2 to 3 generations with or without continuous exposure to a chemical mutagen, and population growth rates in both conditions are compared. Briefly, for each assay plate, we added a consistent amount of bacterial food at high concentration and an isogenic population of synchronized L1 worms. We then imaged the plates continuously on flatbed scanners until the population size increased about 1 million-fold and the food was depleted from the plates. Because bacterial growth, and thereby worm food supply, might be affected by mutagen exposure as well, we fixed the bacteria with a quick, light paraformaldehyde treatment followed by washes. This preserved the bacteria cell shape—a requirement for some nematodes to successfully feed (27, 28). The number of hours it took each plate to exhaust its food is a proxy measurement for population growth rate broadly, and population growth rate is an umbrella fitness phenotype that we chose hoping to capture as many possible contributing fitness phenotypes as might be relevant (e.g., brood size, time of onset of reproductive maturity, lifespan, body size, embryonic viability, mutation burden, etc.).

We used this multigenerational isogenic population growth rate assay to test the sensitivities of 21 isolates [20 strains described above plus CEW1, the reference strain for *O. tipulae* (21)] to three mutagens; cisplatin, ethyl methanesulfonate (EMS), and hydroxyurea (HU). Mutagens were chosen for their variety in DNA damage mechanisms, with EMS primarily causing alkylation (29), cisplatin causing inter- and intrastrand cross-links (30), and HU causing replication fork stalling via depletion of nucleotides (31). For all three mutagens, strains differed in sensitivity (Fig. 5 and *SI Appendix*, Fig. S13). We detected highly significant broad-sense

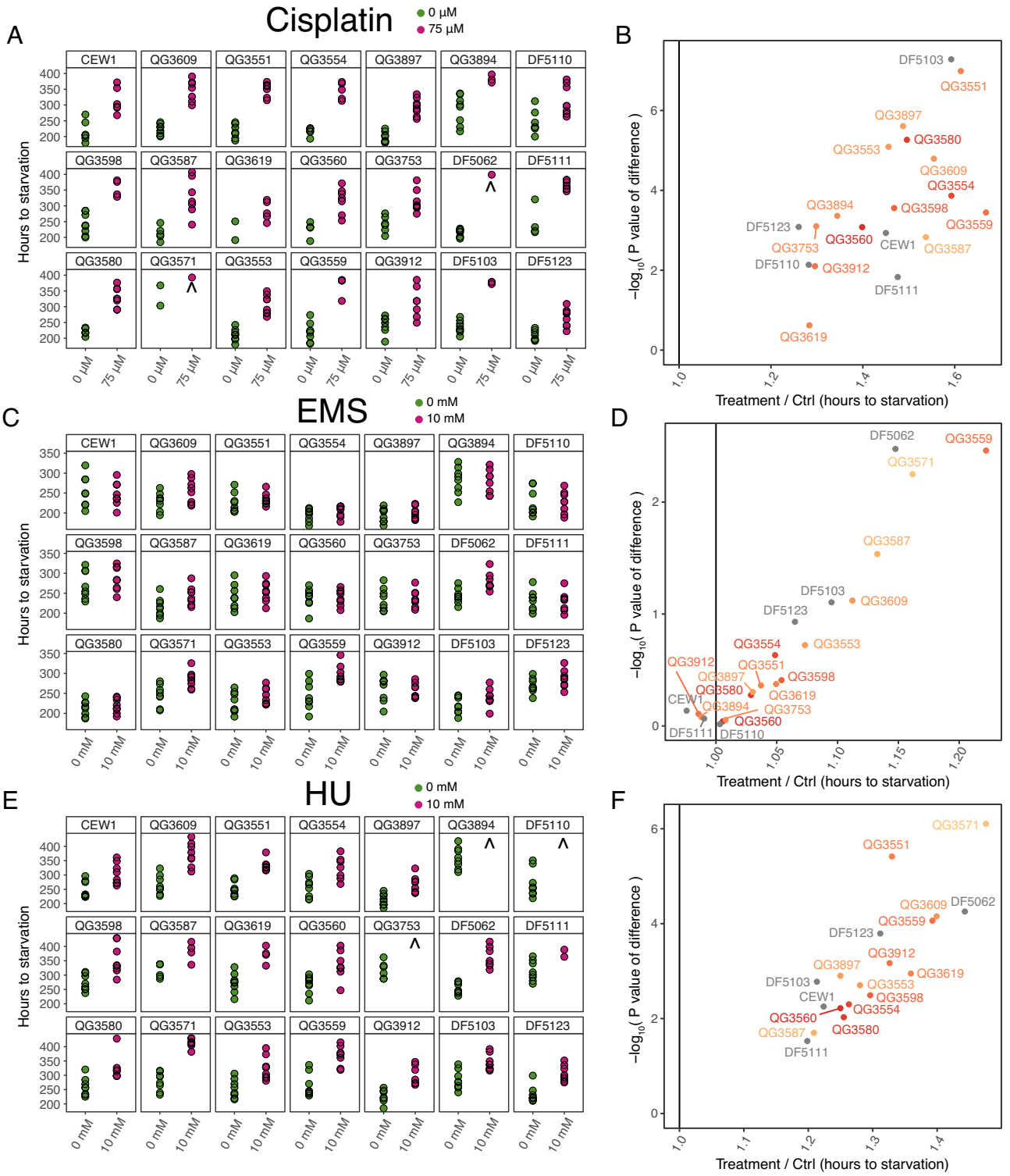

Fig. 5. Mutagen tolerance assays of 21 strains of *O. tipulae* to three mutagens: cisplatin (*A* and *B*), EMS (*C* and *D*), and HU (*E* and *F*). (*A*, *C*, and *E*) Hours of population growth until all food was consumed in cultures without mutagen (green) or with mutagen (pink). (*B*, *D*, and *F*) Ratios of average hours to starvation for mutagen-treated cultures compared to control cultures. Strains plotted further to the right are more sensitive, and strains plotted higher on the *y*-axis are more reproducibly sensitive. Carets in the *Left* panels indicate strains for which 0 or 1 isogenic cultures consumed all the food on the plates with mutagen before the experiment was terminated. These strains do not appear in plots on the *Right* because their *P*-values are undefined.

heritability for sensitivity (H^2_{sens} = 0.37, 0.14, and 0.21 for cisplatin, EMS, and HU, $P < 10^{-10}$ in all cases). However, we found no significant effects of Chornobyl versus non-Chornobyl origins (glm *P*-values for cisplatin = 0.596, EMS = 0.623, HU = 0.421), and no significant association with radioactivity among Chornobyl samples (glm *P*-values for cisplatin = 0.278, EMS = 0.144, HU = 0.155, *SI Appendix*, Fig. S14). While mutagen tolerance cannot be broadly explained by the environment at the time and place of collection, there are nonetheless many interesting anecdotal observations from the intersection of these genomic and mutagen tolerance datasets (*Discussion*), each of which can be pursued directly by genetic and cell biological experimentation in these strains.

Of the two sets of closely related pairs described at the end of the previous section, while the distribution of variants between them was unequal, none of these four strains were exceptionally tolerant or sensitive to the three mutagens tested (Fig. 5). Therefore, we were not able to attribute this difference in mutation acquisition in the wild to broadly applicable differences in mutagen tolerance, and consider it more likely that this discrepancy is due to differences in the strains' exposure history or demography.

Nematodes are highly robust animals, with some species reported as especially tolerant to harsh environmental conditions (32–34). To test whether *O. tipulae* is a singularly tolerant species, we performed the same mutagen sensitivity assay at a range of concentrations in multiple strains of both *O. tipulae* and *C. elegans*, a species we did not find in the CEZ. *C. elegans* showed slightly higher tolerance to cisplatin, comparable tolerance to EMS, and slightly lower tolerance to HU (*SI Appendix*, Fig. S15), leading us to conclude that *O. tipulae* is not an exceptionally mutation-resistance species of rhabditid nematode.

Discussion

Microfauna from polluted or otherwise challenging environments provide valuable opportunities to investigate the nature of resilience and vulnerability within genetically diverse populations. These studies are often observational, as hypotheses and conclusions drawn from the field are not always testable within those same systems in the lab. In this study, we characterized wild nematodes from sites of varying radioactivity within the CEZ, in the field and in the lab. We sequenced and analyzed the genomes of these isolates to investigate the genetic impacts of their recent environmental exposure, we cryopreserved cultures of each isolate, and we established a method for studying differences in tolerance to chronic exposure in this genetically manipulable species.

Many Taxa of Nematode Are Abundant in the CEZ. We successfully isolated nematodes from sites of all levels of radioactivity throughout the CEZ. This may not be surprising—nematodes are robust animals with many life history traits that can be advantageous in a hostile environment. Nevertheless, their reliable abundance in the wild and their experimental tractability position them well as a system that is portable between the field and the lab.

O. tipulae emerged from our collections as the most abundant species from a broad range of environments. Also intriguing was the cephalobe *Acrobeloides*, which we collected in the highest frequency from the most radioactive sites. Parthenogenetic, and with a generation time of about a month, *Acrobeloides* is less amenable to experimentation. But it has been previously described as a highly stress-tolerant animal (32–34) and may be interesting for future studies. Because the highest radiation sites for our collections were also distinctive in other ways (dry, exposed, and sandy), the prevalence of *Acrobeloides* is not evidence that they are adapted to radiation.

No Evidence of Chornobyl-Specific Impacts on the Genomes of *O. tipulae*. The genomes we assembled de novo from long- and short-read data revealed only a single large inversion, in a non-Chornobyl strain, suggesting that exposure-induced chromosomal rearrangements are not common in this population. Inspecting genomes for differential rates of smaller and more numerous mutations is not trivial, as counting private mutations in each strain would largely reflect the population structure of our samples, comparing each strain to a distant outgroup dilutes any effects of post-1986 exposure, and methods that use the full ancestral recombination graph require strong assumptions about unmeasured parameters.

We designed a strategy that compares the relative number of private mutations between each pair of strains, allowing us to identify which branch has acquired more mutations and which fewer in same periods of unshared history, for each pair. The results did not correlate with radiation levels at the collection site.

Previous experiments in *C. elegans* offer some context for this result: Maremonti et al. (25) reported a decrease in brood size due to an increase in apoptosis during spermatogenesis at 40.8 mGy/h but did not see this effect at 10.8 mGy/h (40× and 10× higher dose rates than any of the Chornobyl sites in this study, respectively). This is a dramatic phenotype that can be seen in one animal in one generation, leaving it ambiguous whether there are more subtle effects at lower doses that are nonetheless capable of driving selection. Quevarec et al. showed that this is indeed true, as population sizes decrease at 50 mGy/h (35) but male frequency increases at a lower, Chornobyl-comparable dose of 1.4 mGy/h (36). Other studies are harder to compare to ours, as only Maremonti et al. and Quevarec et al. used chronic exposure (≥72 h), rather than the more commonly studied acute exposure. In one such acute exposure study, Volkova et al. (37) exposed *C. elegans* to 2.14 Gy/min (about 2,000× higher than the Chornobyl sites) for total doses ranging from 0 to 80 Gy, and reported a linear increase in mutation accumulation across this range. The lower and more environmentally relevant end of this range is not well resolved, leaving it unclear at what point this linear mutation accumulation response begins. Furthermore, the relationship between mutation accumulation rates and fitness in wild nematodes is not currently well understood. Wang et al. (38) reported an increase in progeny lethality at as little as 10 Gy exposure during the end of the 4th larval stage in wild-type hermaphrodites, though the dose rate was not specified. Their consistent observation at all doses tested (10 Gy to 120 Gy) that the effect on progeny lethality is greater in the following generation strengthens our conviction that studying chronic exposure over multiple generations provides a more biologically relevant perspective on fitness.

While our experimental design is well suited to address differences between samples within the CEZ, the relatively long branch lengths between non-Chornobyl samples make it challenging to compare Chornobyl to non-Chornobyl populations. Future studies should consider a sampling strategy with similarly closely related non-Chornobyl samples.

Finally, it is not known how quickly worms are migrating around the CEZ due to phoresy, though our PCA shown in Fig. 2*C* suggests that there is little population structure between this area and Berlin. This leaves open the possibility that *Oscheius* nematodes are sensitive to these upper ranges of radioactivity, but that we are sampling worms that have only recently arrived to the high-radiation areas. Regardless, our relative mutation acquisition analysis does point us toward specific strains of interest, which are elaborated on in the next section.

Mutagen Tolerance Varies Heritably among Strains, but Chornobyl Nematodes Do Not Show Exceptional Mutagen Tolerance. One of the many appeals of the nematode as an experimental model is its versatility: It is a rare genetic system that is well suited for studying individual cells, the entire animal, or populations of many millions of animals, all easily and affordably, within the lab. In this study, we use a set of wild nematodes to bridge field work and lab experiments, by culturing Chornobyl strains and assaying their mutagen tolerance in a controlled setting. Comparing population growth over multiple generations in the presence or absence of three mutagens revealed heritably

divergent responses to each mutagen. The fact that these responses vary independently of radiation levels at the site of collection suggests that the radiation these worms were exposed to likely did not surpass the limit of what standing variation in the *O. tipulae* population is equipped to survive. The possibility remains, though, that there are ionizing radiation-specific tolerance mechanisms selected for in Chornobyl that would be missed when testing for mutagen tolerance with the chemicals we used in this study.

By combining results from recent mutation acquisition in the field and mutagen tolerance experiments in the lab, several strains emerge as interesting for further study separately and in comparison. For each mutagen, we now have relatively tolerant and relatively sensitive strains identified, between which we can compare the genetics and DNA integrity dynamics in response to mutagen exposure.

Materials and Methods

Nematode Collection and Identification. We measured ambient radiation at each collection site by Geiger counter (Internal Medcom Inspector), averaging three measurements, each 1 cm above the ground and at least 30 cm from the others. To measure substrate radioactivity, we first estimated each sample's moisture content by weighing the substrate, dehydrating with short pulses in a microwave or by leaving in an oven set to 38 °C for 30 min at a time, and weighing again. Each sample was considered fully dehydrated once heat treatments stopped producing changes in weight. We then used a SAM940 portable gamma spectrometer (Berkeley Nucleonics Corp) with a 10 × 10 cm NaI detector to count Cs137 emissions. Gamma counts were performed inside a lead-brick enclosure to reduce background to under 10 counts per minute, and background was then subtracted from the sample spectrum. Counts were converted to corrected Becquerel as in ref. 39.

All CEZ nematodes were collected using the Baermann funnel technique (40) conducted in Chornobyl within a day of sample collection. Taxonomic assignments are based on 18S sequence similarity to nematodes in the NCBI nucleotide database. A region of 18S was amplified and sequenced using RHAB1350F (5′-TACAATGGAAGGCAGCAGGC) and RHAB1868R (5′-CCTCTGACTTTCGTTCTTGATTAA) primers (41). The gene tree in Fig. 1*B* was generated by aligning 18S sequences in R (42) using msa() from the *msa* package (43) with default settings, then using *ape* (44) to calculate distances (dist.dna(model = "raw", pairwise.deletion = T)), estimate a tree (njs()), root the tree with the *Plectus minimus* sequence (root()), and plot (plot.phylo()).

Long-Read DNA Sequencing. Worms were grown on 10 10-cm plates at 20 °C on high-agarose nematode growth media (NGMA), washed for 1 h in M9, then quickly washed with sterile distilled water, pelleted, and resuspended in 5× volume lysis buffer (200 mM NaCl, 100 mM Tris-HCl pH 8.5, 50 mM ethylenediaminetetraacetic acid (EDTA) pH 8.0, 0.5% sodium dodecyl sulphate (SDS), and 0.1 mg/mL proteinase K added fresh). Worms were lysed at 65 °C for 3 to 12 h and then incubated at 95 °C for 20 min. RNase A was added at 0.1 mg/mL and incubated for 1 h at 37 °C. DNA was isolated by mixing the sample, phenol, chloroform, and isoamyl alcohol in 50:25:24:1 proportions and shaking for 20 s, then spinning down in phase-lock gel tubes for 1 min at 4,000 rcf, followed by 5 min at 16,000 rcf, and keeping the top aqueous phase. Ethanol precipitation was performed by adding 0.1× volume 3 M NaAc and inverting, then adding 1 mL (or >2× total volume) 100% ethanol, mixing, incubating for 20 min at 4 °C, centrifuging for 30 min at 4 °C at 16,000 rcf, removing the supernatant, washing the pellet twice with 70% EtOH, then drying the pellet, and resuspending the DNA overnight in 100 μL water. Size selection was performed with the Short Read Eliminator Kit (Circulomics #SS-100-101-01) according to the manufacturer's instructions. Purified DNA was prepared and sequenced using the Oxford Nanopore Technology MinION device (Ligation Sequencing Kit SQK-LSK110, Spot on flow cell Mk1 FLO-MIN106D, and Native Barcoding Expansion EXP-NBD104) according to the manufacturer's instructions.

Short-Read DNA Sequencing. DNA was extracted by salting out (45). Worms were rinsed in M9 for 1 h then pelleted and frozen overnight. The pellets were thawed and incubated in 275 μL TNE with 7.5 μL 20% SDS and 15 μL 20 mg/mL proteinase K at 55 °C overnight. The next day samples were vortexed, another 15 μL proteinase K was added, and samples were incubated at 55 °C for another 2 h. After 6 μL 100 mg/mL RNase A was added, samples were vortexed and let rest for 2 min. 85 μL 5 M NaCl was added, and samples were shaken vigorously. Samples were spun at 14,000 rpm for 10 min, and the supernatant was moved to a fresh tube. 350 μL ice-cold EtOH was added, and tubes were inverted and then spun at 14,000 rpm for 3 min. The supernatant was removed, and the pellet was dried and resuspended in 20 to 100 μL Tris-EDTA (TE) buffer at 37 °C for a few hours. DNA was passed through a Genomic DNA Clean & Concentrator kit (Zymo D4065) and prepared for sequencing using the NEBNext FS DNA Library Prep Kit (E7805) according to the manufacturer's instructions. Libraries were sequenced on a NextSeq 500 for 2 × 150 cycles at the NYU GenCore Facility.

Genome Assembly. Bases were called and barcoded from MinION data using Oxford Nanopore's guppy/4.4.0_gpu (guppy_basecaller with a minimum qscore of 7, guppy_barcoder). Contigs were assembled with Flye v2.8.1 (flye –nano-raw –genome-size 60m –iterations 1 –meta) (46) and then cleaned with Oxford Nanopore's Medaka (medaka_consensus -m r941_in_high_g360) and Racon v 1.4.19 (47) using default settings. Illumina reads were aligned to post-Racon assembly using minimap2/2.17 (minimap2 -ax sr) (48), and alignments were used to polish assemblies with pilon-1.24 (pilon –geno) (49). Polished contigs were inspected using blobtools v1.1 (map2cov, create, view, and plot) (50), and contigs that were likely contaminants due to their copy number and/or GC content were excluded manually from the final assembly. In three cases, chromosomes were assembled in what appeared to be chromosomal fusions, but inspection of long-read alignments revealed zero reads that spanned nontelomeric regions of both sides of the fusion, so this was inferred to be an assembly error and contigs were manually split.

Genetic Distance, PCA, Mantel Test, Nucleotide Polymorphism, and Genetic Diversity. We subsampled Illumina reads for each isolate's genome so that all libraries had similar coverage (~29×). These subsetted Illumina reads for each sample were aligned to CEW1 reference genome using minimap2 v2.17 and samtools v1.11 (48, 51) (minimap2 -ax sr -R [manually added readgroup], samtools view -S -b, samtools sort, samtools index). Alignments were genotyped and converted to vcfs using GATK v4.3.0.0 (HaplotypeCaller -ax sr to generate GVCFs, GenomicsDBImport to combine all samples into one database, GenotypeGVCFs -all-sites to produce a vcf) (52).

Genetic distances were generated by selecting two strains at a time, filtering them for only sites in which both samples had a read depth >5, and counting the fraction of sites that differed between the pair using bcftools v1.14 (53) (bcftools view -s strain1, strain2 -m 2 -M 2 -i 'MIN(FMT/DP)>5'). PCA was performed using sites for which all samples had a read depth >5. Mantel tests were performed using the adegenet (54) R package command mantel.randtest() on genetic distance calculated above and haversine geographic distance calculated with the geosphere (55) package (distHaversine()).

Watterson's theta (nucleotide polymorphism) was calculated in R by dividing the number of varying sites by the number of sites at which all 20 samples had a read depth greater than 5, for 1 Mb windows centered every 1 Kb. This ratio was divided by the sum of 1/i for i = (1-19). Pi (genetic diversity) was calculated using VCFtools v.0.1.16 (–window-pi 10000) on the VCF of all Chornobyl or all non-Chornobyl samples, aligned to the CEW1 reference genome, subsampled to achieve comparable sequencing depth, and filtered for only for sites with a read depth of at least 5 for all samples.

Synteny Plots. Synteny plots were generated by aligning assembled genomes to the CEW1 reference genome or to each other with minimap2 v2.17 (minimap2 -x asm20) (48) and were plotted in R using the package pafr (56).

Relative Mutation Acquisition. We subsampled Illumina reads for each isolate's genome so that all libraries had similar coverage (~29×). We then aligned reads to the JU75 genome (outgroup *O. sp 3*) or the CEW1 genome (*O. tipulae* reference) using minimap2 v2.17. We called SNPs and indels with GATK v4.1.9.0 (HaplotypeCaller -ax sr, GenomicsDB, GenotypeGVCFs).

To avoid including genomic regions for which DF5123 might not be a suitable outgroup, we broke the full vcf table into 1,000-variant pieces and generated a distance matrix for each piece. If a set of 1,000 variants generated any DF5123 distances that were less than any non-DF5123 distances, we

excluded all 1,000 variants from this analysis. By this method, we removed 22% of variants.

For each possible pair of samples, we made a vcf of those two strains plus DF5123 (the intraspecies outgroup) mapped to CEW1 (the annotated reference strain for *O. tipulae*). We filtered for only sites with two alleles and a minimum read depth of 5 (bcftools v1.14, bcftools -s strain1, strain2 -m 2 -M 2 -i 'MIN(FMT/DP)>5'). From this pruned and filtered vcf, we calculated the ratio of mutations unique to each sample for all mutations or each mutation type separately, added 50 counts to each to buffer against inflated effects of small numbers, and then divided the counts from strain 1 by the counts from strain 2 to generate a relative mutation acquisition value.

The Mantel test was performed using the adegenet (54) R package command mantel.randtest(nrepet=999) on ambient radiation fold change and relative mutation acquisition value for each comparison in both directions.

Analyses were replicated using tandem repeat abundance. Tandem repeats were identified from CEW1 and DF5123 genomes using HipSTR v.4.09.1 (trf409.linux64 [genome.fa] 2 7 7 80 10 50 500 -h -d -l 6 -ngs) as recommended in the HipSTR manuscript and github tutorial (57).

Power Analysis. We simulated 1,000 datasets for the fraction of the genome analyzed in Fig. 4 (regions of the genome for which the DF5123 strain is a suitable outgroup for the Chernobyl and Berlin strains) as follows. For a given mutation rate multiplier (2, 5, or 10), we calculated the expected number of extra mutations each strain would have, given the radioactivity at the site of collection, if 1 Sv/y increased the mutation rate by the specified multiplier value, 10 mSv/y and lower had no increased mutation rate, and mutation rate increased linearly between 10 mSv/y and 1 Sv/y. We assumed a baseline mutation rate of 9.125 mutations per analyzed region of the genome (40 MB) per year, based on data for *C. elegans* supporting a mutation rate of 22.8125 mutations per year (2.5×10^{-9} mutations per base per generation $\times 10^8$ bases * 365/4 generations per year) when reproducing continuously (58, 59). We used these additional mutations to adjust the terminal branch lengths on each of the 1,491 genealogies we had estimated from 1,000 consecutive variants each and then simulated a new set of 1,000 variants for each adjusted tree, resulting in 1,491,000 variants per simulation. We then performed the relative mutation acquisition analysis on each simulation as described above to determine the percent of simulation for which a significant association between radioactivity and relative mutation acquisition was detected.

Fixing Food for Mutagen Experiments. Bacterial cultures of *E. coli* NA22 were grown in Terrific Broth overnight at 37 °C, and *Ochrobactrum vermis* MYb71 (60) were grown in Terrific Broth at 25 °C for two nights, all in 1-L beveled flasks. Cultures were spun down in a Sorvall floor centrifuge in 1-L bottles at 5,000 rpm for 10 min. Pellet weights were determined by weighing empty Sorvall bottles before adding medium and weighing them again after spinning down and removing the supernatant. Pellets were resuspended in sterile water 3× the mass of the pellet. Paraformaldehyde was added to reach a final concentration of 5% and incubated shaking at 37 °C for 1 h. The solution was spun down again in a Sorvall centrifuge, this time in 50 mL tubes, and once again resuspended in 3× the mass of the pellet using sterile water. These two stocks of fixed bacteria were mixed together in a 1:1 ratio by volume to produce the final food stock for mutagen sensitivity assays.

Mutagen Sensitivity Assay. Worms were maintained at 20 °C on NGMA plates seeded with OP50 *E. coli*. Gravid adults were bleached on day 1, and embryos were plated without food to induce L1 arrest. On day 2, synchronized larvae were counted by averaging the number of larvae and late-stage embryos per 1 μL drop for 3 drops, and roughly 50 worms were added to each 3.5 cm NGMA plate with 10 μg/mL nystatin and 50 μg/mL streptomycin. Eight plates of the negative control condition and eight plates of the experimental treatment condition were prepared for each strain. Stocks of fixed NA22 and MYb71 bacteria (see above) were mixed 1:1 by volume, and mutagen solutions (resulting in final concentrations 75 μM cisplatin, 10 mM EMS, or 10 mM HU) or water (for controls) were added to aliquots, 200 μL of which were then distributed onto each plate. Concentrations of mutagens were calculated based on a final volume of the entire 35-mm NGMA plate (3.31 mL), assuming that the mutagen is diffused through the entire plate for the majority of the experiment. Plates were randomized and arranged on acrylic racks on Epson V750, V800, and V850 flatbed scanners in a 20 °C incubator. Acrylic racks held 32 plates in place on each scanner, with 9 mm ventilation below and 4.5 mm ventilation above plates. Scanners collected 1,200 dpi images once per hour continuously until all plates had starved or begun to dry out, usually 10 d for *C. elegans* and 20 d for *O. tipulae*. We used ImageJ to calculate the standard deviation (SD) of pixel intensities for each image, with higher worm-density images having a more bimodal pixel intensity distribution, and therefore a higher standard deviation of pixel intensities. SD values were analyzed in R to determine the exact time of food depletion, which was recognizable by with the abrupt end of exponential population growth and sudden drop in SD of pixel intensity.

Statistics for Mutagen Sensitivity Assay. We estimated broad-sense heritability of toxin sensitivity using a linear mixed-effect model (61). We used the number of hours until each plate was exhausted of food for our phenotype in the model, and the data (after censoring plates that became contaminated or never reached starvation) include 18 to 21 strains measured on 1 to 8 plates per strain per treatment, randomized across eleven flatbed scanners, all assayed in a single experimental batch for each toxicant. Fixed effects are the hours-to-starvation intercept and the effect of treatment (toxin versus control). Random effects are worm strain (random intercepts), treatment effect within strain (random slopes), experimental scanner (random intercepts), and residual microenvironmental variation. The plate-level broad-sense heritability of sensitivity is the fraction of random-effect variance attributed to treatment within strain (i.e., variance explained by the random slopes). Note that among-strain variation in baseline population growth rates (i.e., variance explained by random strain intercepts) accounts for an additional 0.27, 0.37, and 0.26 of the random-effect variance in the cisplatin, EMS, and HU experiments, respectively.

We tested the significance of the heritability of sensitivity by comparing models with and without random slopes, using likelihood ratio tests and the Chi-square distribution to estimate *P*-values.

Data, Materials, and Software Availability. All data and code used to generate the results in this manuscript are available at github.com/tintori/chornobyl_genomes (62). Raw and processed sequencing files are available at NCBI under Project Accession # PRJNA974388 (63).

ACKNOWLEDGMENTS. We thank Maxim Ivanenko for sharing his invaluable expertise in the field, Jonny Turnbull for help collecting nematodes, and Karin Kiontke for help interpreting 18S sequences. We thank Erik Andersen, Ryan Baugh, members of the Andersen, Baugh, and Rockman labs, Sevinç Ercan, and Molly Przeworski for helpful conversations. We thank the NYU Rhabditid Collection for all DF *Oscheius* strains, Marie-Anne Félix for the JU75 strain, and the *Caenorhabditis* Genetics Center for bacterial strains NA22 and MYb71. This work was supported by NIH grant ES031364 (M.V.R.), NIH grant ES029930 (M.V.R.), NIH grant GM141906 (M.V.R.), Damon Runyon Cancer Research Foundation DRG-2371-19 (S.C.T.), Samuel Freeman Charitable Trust (T.A.M.), Zegar Foundation (NYU GenCore), and NIH Office of Research, Infrastructure Programs P40 OD010440 (Caenorhabditis Genetics Center).

1. A. Cheong, Z. D. Nagel, Human variation in DNA repair, immune function, and cancer risk. *Front. Immunol.* **13**, 899574 (2022).
2. V. Tiwari, D. M. Wilson III, DNA damage and associated DNA repair defects in disease and premature aging. *Am. J. Hum. Genet.* **105**, 237–257 (2019).
3. D. E. Cook, S. Zdraljevic, J. P. Roberts, E. C. Andersen, CeNDR, the *Caenorhabditis elegans* natural diversity resource. *Nucleic Acids Res.* **45**, D650–D657 (2017).
4. T. C. Dockendorff *et al.*, The nematode *Oscheius tipulae* as a genetic model for programmed DNA elimination. *Curr. Bio.l* **32**, 5083–5098.e6 (2022).
5. D. H. A. Fitch, K. Kiontke, W. Sudhaus, Rhabditinadb ver. beta 0.92 (2023). https://wormtails.bio.nyu.edu.
6. R. Ghosh, E. C. Andersen, J. A. Shapiro, J. P. Gerke, L. Kruglyak, Natural variation in a chloride channel subunit confers avermectin resistance in *C. elegans*. *Science* **335**, 574–578 (2012).
7. L. M. Noble *et al.*, Polygenicity and epistasis underlie fitness-proximal traits in the *Caenorhabditis elegans* multiparental experimental evolution (CeMEE) panel. *Genetics* **207**, 1663–1685 (2017).
8. S. J. Widmayer, T. A. Crombie, J. N. Nyaanga, K. S. Evans, E. C. Andersen, *C. elegans* toxicant responses vary among genetically diverse individuals. *Toxicology* **479**, 153292 (2022).
9. A. P. Moller, K. A. Hobson, T. A. Mousseau, A. M. Peklo, Chernobyl as a population sink for barn swallows: Tracking dispersal using stable-isotope profiles. *Ecol. Appl.* **16**, 1696–1705 (2006).
10. Z. Boratynski *et al.*, Ionizing radiation from Chernobyl affects development of wild carrot plants. *Sci. Rep.* **6**, 39282 (2016).

11. A. P. Moller, J. Erritzøe, F. Karadas, T. A. Mousseau, Historical mutation rates predict susceptibility to radiation in Chernobyl birds. *J. Evol. Biol.* **23**, 2132–2142 (2010).
12. R. J. Baker *et al.*, Elevated mitochondrial genome variation after 50 generations of radiation exposure in a wild rodent. *Evol. Appl.* **10**, 784–791 (2017).
13. C. Car *et al.*, Unusual evolution of tree frog populations in the Chernobyl exclusion zone. *Evol. Appl.* **15**, 203–219 (2022).
14. M. N. Dillon *et al.*, Population dynamics and genome-wide selection scan for dogs in Chernobyl. *Canine Med. Genet.* **10**, 1 (2023).
15. H. Ellegren, G. Lindgren, C. R. Primmer, A. P. Moller, Fitness loss and germline mutations in barn swallows breeding in Chernobyl. *Nature* **389**, 593–596 (1997).
16. J. Kesaniemi *et al.*, Analysis of heteroplasmy in bank voles inhabiting the Chernobyl exclusion zone: A commentary on baker et al. (2017) "elevated mitochondrial genome variation after 50 generations of radiation exposure in a wild rodent". *Evol. Appl.* **11**, 820–826 (2018).
17. G. J. Spatola *et al.*, The dogs of Chernobyl: Demographic insights into populations inhabiting the nuclear exclusion zone. *Sci. Adv.* **9**, eade2537 (2023).
18. M. Yeager *et al.*, Lack of transgenerational effects of ionizing radiation exposure from the Chernobyl accident. *Science* **372**, 725–729 (2021).
19. D. Kahle, H. Wickham, ggmap: Spatial visualization with ggplot2. *The R J.* **5**, 144–161 (2013).
20. M.-A. Félix, "Oscheius tipulae" in *WormBook: The Online Review of C. elegans Biology*, The C. elegans Research Community, Ed. (WormBook, 2006), 10.1895/wormbook.1.119.1.
21. P. M. Gonzalez de la Rosa *et al.*, A telomere-to-telomere assembly of *Oscheius tipulae* and the evolution of rhabditid nematode chromosomes. *G3 (Bethesda)* **11**, jkaa020 (2021).
22. M.-A. Félix, A. Vierstraete, J. Vanfleteren, Three biological species closely related to *Rhabditis* (*Oscheius*) *pseudodolichura* körner in Osche, 1952. *J. Nematol.* **33**, 104–109 (2001).
23. A. D. Cutter, Nucleotide polymorphism and linkage disequilibrium in wild populations of the partial selfer *Caenorhabditis elegans*. *Genetics* **172**, 171–184 (2006).
24. J. G. Tate *et al.*, Cosmic: The catalogue of somatic mutations in cancer. *Nucleic Acids Res.* **47**, D941–D947 (2019).
25. E. Maremonti *et al.*, Gamma radiation induces life stage-dependent reprotoxicity in *Caenorhabditis elegans* via impairment of spermatogenesis. *Sci. Total Environ.* **695**, 133835 (2019).
26. N. Stroustrup *et al.*, The *Caenorhabditis elegans* lifespan machine. *Nat. Methods* **10**, 665–670 (2013).
27. C. Fang-Yen, L. Avery, A. D. Samuel, Two size-selective mechanisms specifically trap bacteria-sized food particles in *Caenorhabditis elegans*. *Proc. Natl. Acad. Sci. U.S.A.* **106**, 20093–20096 (2009).
28. M. R. Flavel *et al.*, Growth of Caenorhabditis elegans in defined media is dependent on presence of particulate matter. *G3 (Bethesda)* **8**, 567–575 (2018).
29. G. A. Sega, A review of the genetic effects of ethyl methanesulfonate. *Mutat. Res.* **134**, 113–142 (1984).
30. J. D. S. Orbell, C. Solorzano, L. G. Marzilli, T. J. Kistenmacher, Preparation and structure of cis-chlorodiammine(n2, n2-dimethyl-9-methylguanine)platinum(ii) hexafluorophosphate. A model for the intermediate in the proposed crosslinking mode of action of platinum(ii) antitumor agents. *Inorg. Chem.* **21**, 3806–3810 (1982).
31. A. Kurose *et al.*, Effects of hydroxyurea and aphidicolin on phosphorylation of ataxia telangiectasia mutated on ser 1981 and histone h2ax on ser 139 in relation to cell cycle phase and induction of apoptosis. *Cytometry A* **69**, 212–221 (2006).
32. A. F. Bird, M. H. Ryder, Feeding of the nematode *Acrobeloides nanus* on bacteria. *J. Nematol.* **25**, 493–499 (1993).
33. Y. Demeure, D. W. Freckman, S. D. Van Gundy, Anhydrobiotic coiling of nematodes in soil. *J. Nematol.* **11**, 189–195 (1979).
34. A. W. Van der Wurff *et al.*, Type of disturbance and ecological history determine structural stability. *Ecol. Appl.* **17**, 190–202 (2007).
35. L. Quevarec *et al.*, Ionizing radiation affects the demography and the evolution of *Caenorhabditis elegans* populations. *Ecotoxicol. Environ. Saf* **249**, 114353 (2023).
36. L. Quevarec *et al.*, Male frequency in *Caenorhabditis elegans* increases in response to chronic irradiation. *Evol. Appl.* **15**, 1331–1343 (2022).
37. N. V. Volkova *et al.*, Mutational signatures are jointly shaped by DNA damage and repair. *Nat. Commun.* **11**, 2169 (2020).
38. S. Wang, D. H. Meyer, B. Schumacher, Inheritance of paternal DNA damage by histone-mediated repair restriction. *Nature* **613**, 365–374 (2023).
39. A. Lavrinienko, E. Tukalenko, T. Mappes, P. C. Watts, Skin and gut microbiomes of a wild mammal respond to different environmental cues. *Microbiome* **6**, 209 (2018).
40. S. C. Tintori, S. A. Sloat, M. V. Rockman, Rapid isolation of wild nematodes by baermann funnel. *J. Vis. Exp.* **179**, 10.3791/63287 (2022).
41. M. Haber *et al.*, Evolutionary history of *Caenorhabditis elegans* inferred from microsatellites: Evidence for spatial and temporal genetic differentiation and the occurrence of outbreeding. *Mol. Biol. Evol.* **22**, 160–173 (2005).
42. R Core Team, R: A Language and Environment for Statistical Computing (Version 4.2.1, R Foundation for Statistical Computing, Vienna, Austria, 2020). https://www.R-project.org/.
43. U. Bodenhofer, E. Bonatesta, C. Horejs-Kainrath, S. Hochreiter, Msa: An r package for multiple sequence alignment. *Bioinformatics* **31**, 3997–3999 (2015).
44. E. Paradis, K. Schliep, Ape 5.0: An environment for modern phylogenetics and evolutionary analyses in r. *Bioinformatics* **35**, 526–528 (2019).
45. P. Sunnucks, D. F. Hales, Numerous transposed sequences of mitochondrial cytochrome oxidase i–ii in aphids of the genus *sitobion* (hemiptera: Aphididae). *Mol. Biol. Evol.* **13**, 510–524 (1996).
46. M. Kolmogorov, J. Yuan, Y. Lin, P. A. Pevzner, Assembly of long, error-prone reads using repeat graphs. *Nat. Biotechnol.* **37**, 540–546 (2019).
47. R. Vaser, I. Sovic, N. Nagarajan, M. Sikic, Fast and accurate de novo genome assembly from long uncorrected reads. *Genome Res.* **27**, 737–746 (2017).
48. H. Li, Minimap2: Pairwise alignment for nucleotide sequences. *Bioinformatics* **34**, 3094–3100 (2018).
49. B. J. Walker *et al.*, Pilon: An integrated tool for comprehensive microbial variant detection and genome assembly improvement. *PLoS One* **9**, e112963 (2014).
50. D. R. Laetsch, M. L. Blaxter, Blobtools: Interrogation of genome assemblies. *F1000Research* **6**, 1287 (2017).
51. H. Li *et al.*, Genome Project Data Processing. The sequence alignment/map format and samtools. *Bioinformatics* **25**, 2078–2079 (2009).
52. A. McKenna *et al.*, The genome analysis toolkit: A mapreduce framework for analyzing next-generation DNA sequencing data. *Genome Res.* **20**, 1297–1303 (2010).
53. H. Li, A statistical framework for snp calling, mutation discovery, association mapping and population genetical parameter estimation from sequencing data. *Bioinformatics* **27**, 2987–2993 (2011).
54. T. Jombart, Adegenet: A r package for the multivariate analysis of genetic markers. *Bioinformatics* **24**, 1403–1405 (2008).
55. R. J. Hijman, Geosphere: Spherical trigonometry version (R package, 2022). https://CRAN.R-project.org/package=geosphere.
56. D. Winter, Pafr: Read, manipulate and visualize "pairwise mapping format" data (R version, 2020). https://CRAN.R-project.org/package=pafr.
57. T. Willems *et al.*, Genome-wide profiling of heritable and *de novo* str variations. *Nat. Methods* **14**, 590–592 (2017).
58. A. S. Saxena, M. P. Salomon, C. Matsuba, S. D. Yeh, C. F. Baer, Evolution of the mutational process under relaxed selection in *Caenorhabditis elegans*. *Mol. Biol. Evol.* **36**, 239–251 (2019).
59. D. R. Denver *et al.*, Variation in base-substitution mutation in experimental and natural lineages of *Caenorhabditis* nematodes. *Genome Biol. Evol.* **4**, 513–522 (2012).
60. P. Dirksen *et al.*, Cembio–The Caenorhabditis elegans microbiome resource. *G3 (Bethesda)* **10**, 3025–3039 (2020).
61. D. Bates, M. Machler, B. M. Bolker, S. C. Walker, Fitting linear mixed-effects models using lme4. *J. Stat. Softw.* **67**, 1–48 (2015).
62. S. Tintori, Chornobyl Genomes. GitHub. https://github.com/tintori/chornobyl_genomes. Accessed 23 August 2023.
63. S. Tintori, Genomes of 20 Oscheius tipulae and 1 O. sp. 3. NCBI BioProject. https://www.ncbi.nlm.nih.gov/bioproject/PRJNA974388/. Accessed 23 August 2023.